Entrapment of Ionic Tris(2,2′-Bipyridyl) Ruthenium(II) in Hydrophobic Siliceous Zeolite: O_2 Sensing in Biological Environments

Toni A. Ruda-Eberenz, Amber Nagy, W. James Waldman, and Prabir K. Dutta*

Departments of Chemistry and Pathology, The Ohio State University, Columbus, Ohio 43210

Received April 17, 2008. Revised Manuscript Received June 5, 2008

Synthesis of the ionic dye, tris(2,2′-bipyridyl) ruthenium(II) chloride ($Ru(bpy)_3^{2+}\cdot 2Cl^-$) within the supercages of a highly hydrophobic zeolite Y is reported. Use of the neutral precursor $Ru(bpy)Cl_2(CO)_2$ allowed for high loading levels of $Ru(bpy)_3^{2+}$ (1 per 7 and 25 supercages). The emission quenching of the $Ru(bpy)_3^{2+}$-zeolite crystals dispersed in polydimethoxysiloxane (PDMS) films by dissolved oxygen in water was examined. The quenching data as a function of oxygen concentration was fit to a linear Stern-Volmer plot ($R^2 = 0.98$). Using the Stern−Volmer plot as calibration, changes in concentration of dissolved oxygen due to reaction with glucose in the presence of glucose oxidase was monitored. Human monocyte-derived macrophages internalized the submicron-sized $Ru(bpy)_3^{2+}$-zeolite crystals, and intracellular oxygen concentrations initiated by zymosan-mediated oxidative burst could be monitored by measuring the emission from $Ru(bpy)_3^{2+}$ by confocal fluorescence microscopy.

Introduction

Optical oxygen sensors find use in a variety of applications that include monitoring oxygen in water, soil, industrial fermentation and sterilization processes, pressure sensitive paints, and biological systems.[1] An active area of research involves monitoring of analytes, including oxygen, within living cells. One strategy is to use an emissive dye molecule, incorporated into a host, with the emission being sensitive to analyte concentration. Fiber optic devices incorporating dye-host systems, with the host typically being a polymer, have been reported for intracellular monitoring. A disadvantage of these devices is the possibility of cellular damage.[2] For dye-based oxygen sensors, issues regarding dye leaching from the support matrix,[3] and nonlinear Stern-Volmer plots due to a heterogeneous distribution of dye molecules within the host need to be addressed.[4] Phospholipid vesicles have been used as hosts,[5] and improved stability of vesicles via cross-linking polymerization of methacrylate units has been reported.[6,7] Recently, PEBBLE (probes encapsulated by biologically localized embedding) sensors based on polymers have shown promise for monitoring intracellular analyte concentrations. PEBBLE sensors offer small size (20−200 nm in diameter) with minimal cell perturbation, fast response, high selectivity, and good reversibility.[8−10]

The present study is focused on using dye-loaded zeolites for monitoring dissolved oxygen. Zeolites are aluminosilicates which provide a crystalline, well-ordered environment for the dye molecules. Typical sizes of these crystallites extend from 20 nm to microns. The cages of zeolites, especially zeolite-Y can be used to securely entrap dye molecules without any leaching from the matrix. The best such example is tris(2,2′-bipyridyl) ruthenium(II) ($Ru(bpy)_3^{2+}$), which has a diameter of about 12 Å, while the supercages of the zeolite-Y have diameters of about 13 Å with 7 Å windows. Therefore, a "ship-in-a-bottle" synthetic scheme to assemble the ruthenium compound inside a zeolite supercage ensures permanent entrapment since the 7 Å windows will not allow the molecule to escape, and yet the dye molecule is accessible to analytes that can enter through the 7 Å windows.[11]

Loading $Ru(bpy)_3^{2+}$ into zeolite-Y is a simple procedure involving ion-exchange of a ruthenium precursor followed by reaction with 2,2′-bipyridine. Such $Ru(bpy)_3^{2+}$/zeolite-Y materials have been examined for detection of oxygen.[12] We have reported that with more siliceous zeolite-Y, the quenching of $Ru(bpy)_3^{2+}$ by dissolved oxygen is enhanced as compared to zeolite-Y (Si/Al = 2.6) because the intrazeolitic water in the latter blocks oxygen transport to the sensitizer.[13] Siliceous zeolite-Y is comprised only of silicon and oxygen making it highly hydrophobic, hence conventional ion-exchange methods to introduce the ruthenium precursor cannot be used with siliceous zeolite-Y. To incorporate $Ru(bpy)_3^{2+}$ in siliceous zeolite-Y (Si/Al > 100), a neutral ruthenium precursor, $Ru(bpy)Cl_3$ soluble in organic solvents was used; however, the loading level of dye was only about 1 ruthenium complex in 10 000 supercages.[14]

The objectives of the present study were to devise a new synthetic strategy that results in controlled loading level of the ionic dye $Ru(bpy)_3^{2+}\cdot 2Cl^-$ in highly hydrophobic siliceous zeolite-Y and to investigate the use of such materials for detecting dissolved oxygen in aqueous media. The ruthenium precursor used is the neutral species $Ru(bpy)(CO)_2Cl_2$, synthesized from $Ru(CO)_3Cl_2$ and 2,2′-bipyridine by methods described in the

* To whom correspondence should be addressed. E-mail: dutta@chemistry.ohio-state.edu.

(1) Amao, Y. *Microchim. Acta* **2003**, *143*, 1–12.
(2) Buhlman, P.; Pretsch, E.; Bakker, E. *Chem. Rev.* **1998**, *98*, 1593–1647.
(3) Cao, Y.; Koo; Yong-Eun, L.; Kopelman, R. *Analyst* **2004**, *129*(8), 745–750.
(4) Carraway, E. R.; Demas, J. N.; DeGraff, B. A.; Bacon, J. R. *Anal. Chem.* **1991**, *63*, 337–342.
(5) McNamara, K. P.; Nguyen, T.; Dumitrascu, G.; Ji, J.; Rosenzweig, N.; Rosenzweig, Z. *Anal. Chem.* **2001**, *73*(14), 3240–3246.
(6) Hotz, J.; Meier, W. *Langmuir* **1998**, *14*(5), 1031–1036.
(7) Cheng, Z.; Aspinwall, C. A. *Analyst* **2006**, *131*, 236–243.
(8) Clark, H. A.; Barker, S. L. R.; Brasuel, M.; Miller, M. T.; Monson, E.; Parus, S.; Shi, Z.-Y.; Song, A.; Thorsrud, B.; Kopelman, R.; Ade, A.; Meixner, W.; Athey, B.; Hoyer, M.; Hill, D.; Lightle, R.; Philbert, M. A. *Sens. Actuators B* **1998**, *51*, 12–16.
(9) Xu, H.; Aylott, J. W.; Kopelman, R.; Miller, T. J.; Philbert, M. A. *Anal. Chem.* **2001**, *73*, 4124–4133.
(10) Koo, Y. E. L.; Cao, Y.; Kopelman, R.; Koo, S. M.; Brasuel, M.; Philbert, M. A. *Anal. Chem.* **2004**, *76*, 2498–2505.
(11) Castagnola, N. B.; Dutta, P. K. *J. Phys. Chem. B* **2001**, *105*, 1537–1542.
(12) Meier, B.; Werner, T.; Klimant, I.; Wolfbeis, O. S. *Sens. Actuators, B* **1995**, *B29*(1−3), 240–245.
(13) Coutant, M. A.; Payra, P.; Dutta, P. K. *Microporous Mesoporous Mater.* **2003**, *60*(1−3), 79–90.
(14) Payra, P.; Dutta, P. K. *Microporous Mesoporous Mater.* **2003**, *64*, 109–118.

10.1021/la801204y CCC: $40.75
Published on Web 07/22/2008

literature.[15] Siliceous zeolite-Y was obtained from a commercial source. We also report the performance of these dye-loaded zeolite particles for measuring intracellular oxygen in macrophage cells during phagocytosis.

Experimental Section

Siliceous Zeolite-Y. Siliceous zeolite-Y was obtained from a commercial source (HSZ-390HUA, Tosoh Corporation, Tokyo, Japan), with a SiO_2/Al_2O_3 ratio of >200. The siliceous zeolite-Y was characterized via solid state nuclear magnetic resonance spectroscopy (SSNMR), X-ray powder diffraction (XRD), scanning electron microscopy (SEM), and Brunauer−Emmett−Teller (BET)-based surface area measurements.

Synthesis of $Ru(bpy)Cl_2(CO)_2$. The synthesis of the ruthenium precursor $Ru(bpy)Cl_2(CO)_2$ followed literature methods.[15] The reagents and solvents used were p.a. grade (p.a.= pro analysis), and the synthesis was performed in an inert atmosphere. One gram of $Ru(CO)_3Cl_2$ was dissolved in 80 mL dry tetrahydrofuran (THF) by refluxing for 2.75 h, and 0.75 g of 2,2′-bipyridine in 20 mL of THF was slowly added to this solution via a syringe. The solution was refluxed for 45 min, cooled to room temperature, placed in a refrigerator for 2−3 days, and a solid was recovered. A second precipitate was collected after 2−3 more days in the refrigerator. Recrystallization was performed with chloroform and ethanol. The precursor was characterized via infrared and NMR spectroscopy.

Synthesis of $Ru(bpy)_3^{2+}$-Siliceous Zeolite-Y. The ruthenium precursor, $Ru(bpy)Cl_2(CO)_2$, was dissolved in acetonitrile and added to the zeolite, the solvent was removed, and sample was heated to 150 °C under vacuum. The tube was sealed off on the vacuum line, and the sample was heated in an oven to 200 °C with an excess amount of 2,2′-bipyridine (∼3.5 bpy/Ru). The excess ligand was removed from the zeolite via Soxhlet extraction with ethanol (4 weeks) and then ion-exchanged with 0.1 M NaCl. Elemental analysis of the ruthenium loaded siliceous zeolite-Y was performed by Galbraith laboratories using ICP-OES.

PDMS−$Ru(bpy)_3$−Siliceous Zeolite-Y Membrane. The polydimethylsiloxane (PDMS) [RTV 615A and RTV 615B] used was obtained from GE Silicones, Wilton, CT, USA. The procedure for incorporating the zeolite was adapted from the literature.[14,16] The $Ru(bpy)_3^{2+}$-siliceous zeolite-Y was dehydrated under vacuum at 110 °C for 12 h. Typically, 0.01 g dehydrated zeolite was mixed with 1.6 g of dry hexane and sonicated for 4−6 h. 0.15 g of RTV 615A and 0.01 g of dry hexane was added to the zeolite and sonicated for 5 h. 0.015 g of RTV 615B was then added and sonicated for an additional 30 min. The mixture was cast onto a glass plate and kept in a vacuum at 60 °C overnight. Film thickness was examined via profilometry using a Veeco Dektak^3 ST.

Emission Quenching. Emission was monitored with a SPEX Fluorolog spectrophotometer. The Ru-loaded zeolite dispersed in the PDMS film/glass slide was placed diagonally in a cuvette filled with deionized (DI) water. The sample was excited at 450 nm and emission spectra recorded over 500−800 nm using right angle geometry.

Gas was bubbled through the water for 15 min prior to measurement. The gases used were oxygen (99.99%), air, a 60/40 mixture of oxygen/nitrogen, and nitrogen (99.999%). The area under the emission peak at 610 nm was analyzed in order to determine percent quenching.

Oxidation of glucose using glucose oxidase was utilized to monitor changes in dissolved oxygen concentration using the zeolite-PDMS film. Glucose oxidase (EC 1.1.3.4 type II−S from *Aspergillus niger* with a specific activity of 47 200 units per gram of solid) made at a concentration of 4.7 U/mL in phosphate buffer at pH 6.5 (SIGMA, St. Louis, MO) was used. Small volumes of a 17.5 mM β-D-glucose (SIGMA, St. Louis, MO) were added in increments to produce solutions of the following glucose concentrations: 0.25, 0.50, 0.75, 1.0 mM. The Stern−Volmer equation was used in order to calculate oxygen concentrations.

Monitoring Emission in Live Cells. *Isolation and Differentiation of Human Monocyte-Derived Macrophages (MDM).* Peripheral blood mononuclear cells (PBMCs) were separated by Ficoll-Hypaque (Histopaque, Sigma) density gradient centrifugation from buffy coats purchased from the American Red Cross as previously described.[17] Because complete donor anonymity is a strict condition of this arrangement, no Institutional Review Board human subjects protocol is required, as specified by the NIH and Ohio State University IRB guidelines. To promote monocyte differentiation into the macrophage phenotype, PBMCs were aspirated from the plasma/Histopaque interface, washed three times in phosphate buffered saline solution (PBS, buffered to pH = 7.4), suspended in RPMI 1640 (GIBCO) supplemented with 10% pooled normal human serum and 0.1% penicillin/streptomycin. Suspended cells were transferred to Teflon plates where they were incubated for 5−7 days at 37 °C in a humidified atmosphere of 5% CO_2/95% air. The cells were then transferred to Laboratory-Tek II 4-well sterile chambered borosilicate coverglass slides (Nalge Nunc International) for confocal microscopy, or Optilux 96-well microtiter plates (Falcon) for luminol assay, and incubated 24 h prior to removal of nonadherent cells as previously described.[18] Monocyte-derived macrophages (MDM) prepared in this manner routinely marked 90−95% positive for CD14 with undetectable levels of $CD3^+$ T cell contamination as determined by immunofluorescence flow cytometry.

Treatment of MDM with Zeolite Particles. Tris(2,2′-bipyridyl) ruthenium(II) loaded siliceous zeolite-Y particles were sterilized by steam autoclave and suspended in PBS at a concentration of 5 mg/mL. Following 2−3 days incubation of MDM in chamber slides, zeolite suspensions were sonicated and added to cell cultures at a concentration of 6 μg/cm^2. Slides were incubated for 24 h to allow internalization of particles, then rinsed with PBS to remove residual uninternalized particles, and supplied with fresh culture medium. To visualize cell nuclei, slides were incubated for 2 h with the fluorescent, DNA-binding dye, 4′,6-diamidino-2-phenylindole (DAPI, Molecular Probes, Inc.), then rinsed and supplied with fresh culture medium. To induce oxidative burst, zymosan (50 μg/cm^2, Sigma) was added prior to observation by scanning confocal microscopy.

Luminol Assay: Oxidative Burst Optimization. To confirm macrophage oxidative burst kinetics, reactive oxygen species generated in response to phorbol 12-myristate 13-acetate or zymosan treatment were measured by luminol assay.[19,20] The following components were added to each of triplicate wells: 100 μL serum-free culture medium, 100 μL luminol (5-amino-2,3-dihydro-1,4-phthalazinedione, sodium salt, Sigma) for a final concentration of 0.5 mM, and either phorbol 12-myristate 13-acetate (20 ng/well) or zymosan (25 μg/well). A set of triplicate control wells containing MDMs, culture medium, and luminol, but no stimulant, were also included in each experiment. All reagents were maintained at 4 °C and plates were kept on ice during addition of reagents. Luminescence was measured immediately on a Top Count Scintillation and Luminescence counter (Packard). The plates were then incubated for 5 to 10 min intervals at 37 °C in a humidified atmosphere of 5% CO_2/95% air, and recounted. This process was repeated over a period of 80 min. Luminescence indices for each time point were calculated by dividing the mean luminescence counts per minute (cpm) of 3 replicate treated wells by the mean cpm of 3 negative control wells.

Confocal Fluorescence Microscopy. All fluorescent images were obtained with a Leica TCS SP2 confocal fluorescence microscope. The tris(2,2′-bipyridyl) ruthenium (II) loaded zeolite was excited at 488 nm, while the DAPI was excited at 350 nm (Coherent Innova 90). Cells were warmed to 37 °C on the microscope stage. Emission was monitored between 600−650 nm for the ruthenium complex

(15) Haukka, M.; Kiviaho, J.; Ahlgren, M.; Pakkanen, T. *Organometallics* **1995**, *14*, 825–833.
(16) Alvaro, M.; Garcıa, H.; Corrent, S.; Scaiano, J. C. *J. Phys. Chem. B* **1998**, *102*, 7530–7534.
(17) Waldman, W. J.; Adams, P. W.; Orosz, C. G.; Sedmak, D. D. *Transplantation* **1992**, *54*, 887–896.
(18) Waldman, W. J.; Kristovich, R.; Knight, D. A.; Dutta, P. K. *Chem. Res. Toxicol.* **2007**, *20*(8), 1149–1154.
(19) Fach, E.; Waldman, W. J.; Williams, M.; Long, J.; Meister, R. K.; Dutta, P. K. *Environ. Health Perspect.* **2002**, *110*(11), 1087–1096.
(20) Long, J. F.; Waldman, W. J.; Kristovich, R.; Williams, M.; Knight, D.; Dutta, P. K. *Environ. Health Perspect.* **2005**, *113*, 170–174.

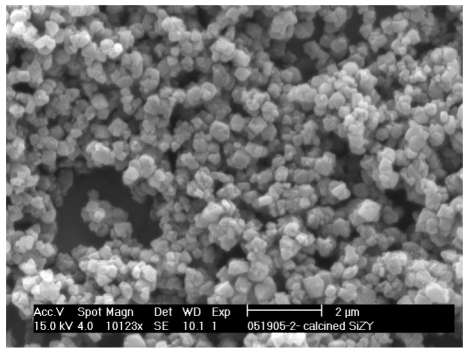

Figure 1. SEM micrograph of siliceous zeolite Y.

and 400−480 nm for the nuclear stain using a photomultiplier tube. Both air and CO_2 atmosphere were used. For cells in a CO_2 atmosphere, a 10 min exposure time was initially allowed before adding the zymosan. Autoclaved zymosan (50 μg/cm^2) was added right before the initial scan in order to induce oxidative burst. Scans were taken every 4 min for 20−28 min. Care was taken not to keep cells in a CO_2 atmosphere beyond 45 min. Data was analyzed with the Leica Confocal software. The luminescence intensity per cell was obtained for both the nuclear stain and the ruthenium complex. For data analysis, all completely visible cells (i.e., cells that were fully in the field being monitored and did not move out of the field during the scan, typically 6−10 cells) were selected.

Results

I. $Ru(bpy)_3^{2+}$-Siliceous Zeolite-Y (RBP-SZY). The siliceous zeolite-Y was found to have a surface area of 775 m^2/g by BET measurement. The solid-state NMR of the sample displays a single strong peak at −107.8 ppm (Figure 1 in Supporting Information), as expected for tetrahedrally bound silicon with no aluminum present ($Si(OSi)_4$)).[21,22] Powder X-ray diffraction shows that the siliceous zeolite is crystalline (data not shown). The SEM of the siliceous zeolite-Y shows the particle size is ∼0.5 μm (Figure 1).

$Ru(bpy)Cl_2(CO)_2$ was used as the precursor for synthesis of intrazeolitic $Ru(bpy)_3^{2+}$. There are three possible $Ru(bpy)Cl_2(CO)_2$ stereoisomers: trans complex (trans Cl ligands, cis CO ligands) (1), cis complex (cis Cl ligands, cis CO ligands) (2), and trans complex (trans CO ligands, cis Cl ligands) (3). Complex (3) is unlikely due to the thermodynamically unfavorable trans position of both carbonyl ligands.[23] The IR data for $Ru(bpy)Cl_2(CO)_2$ (in CH_2Cl_2) shows two ν(CO) stretching bands at 2065(vs) and 2003(vs) cm^{-1} (Figure 2 in Supporting Information). Figure 2 shows the ^{1}H NMR in $CDCl_3$ with peaks at δ 9.8(d), 8.9(d), 8.1(t), 7.8(t), 7.6(t) and several overlapping peaks from 8.0 to 8.3 ppm, and can be assigned to the cis complex (2).[15,24–26] A weak peak due to the trans (1) form can be seen at ∼ 9.2 ppm. Slight impurity of the trans form is not an issue for synthesis of intrazeolitic $Ru(bpy)_3^{2+}$, since both the cis and trans forms of $Ru(bpy)Cl_2(CO)_2$ can enter the zeolite supercages and should have comparable thermochemistry to form the $Ru(bpy)_3^{2+}$.

The synthetic scheme for $Ru(bpy)_3^{2+}$-siliceous zeolite-Y (RBP-SZY) is shown in Scheme 1. $Ru(bpy)Cl_2(CO)_2$ was introduced into a dehydrated zeolite followed by heating with the 2,2′-bipyridine ligand under a closed vacuum. The sample was purified by extensive Soxhlet extraction to remove excess ligand. Since the $Ru(bpy)_3^{2+}$ is ∼13 Å in size compared to the ∼7 Å supercage window, the $Ru(bpy)_3^{2+}$ is not leachable from the matrix. Loading levels of $Ru(bpy)_3^{2+}$ in the zeolite were varied by altering the initial $Ru(bpy)Cl_2(CO)_2$ to zeolite-Y ratio. Two samples were prepared, and elemental analysis was performed on each sample in duplicate. The higher loading level sample showed a loading of one $Ru(bpy)_3^{2+}$ per seven supercages for each analysis. The lower loading level sample showed one result of 1 $Ru(bpy)_3^{2+}$ per 17 supercages, and the other was 1 $Ru(bpy)_3^{2+}$ per 25 supercages. Therefore, the actual loading level is somewhere in between, and we will refer to this sample as 1 $Ru(bpy)_3^{2+}$ per 25 supercages. This sample was used for all studies in this paper. Figure 3A shows the diffuse reflectance spectrum of this sample. The peak around 285 nm arises from the 2,2′-bipyridyl ligand, and the peak at 450 nm is due to the metal to ligand charge transfer (MLCT) band of the intrazeolitic $Ru(bpy)_3^{2+}$.[27]

II. Emission Spectroscopy as a Function of Dissolved Oxygen. The fluorescence spectra of a sample of RBP-SZY placed in nitrogen-saturated versus an oxygen-saturated water solution is shown in Figure 3B. The sample was prepared by dispersing RBP-SZY powder in a PDMS film supported on a glass plate. Film thickness varied from 50−150 μm. The emission from $Ru(bpy)_3^{2+}$ in the RBP-SZY-PDMS film in solutions with varying levels of dissolved oxygen was measured. The solutions were prepared by bubbling N_2, air (21% O_2/N_2), 60% O_2/N_2 and O_2 into water. The overall quenching between a solution of nitrogen-saturated and oxygen-saturated water is about 41% (integrated area 0% $O_2 = 6.4 \times 10^9$; 100% $O_2 = 3.7 \times 10^9$). The Stern−Volmer plot (normalized to nitrogen saturated water, I_o) is shown in Figure 4 and is fit with a linear equation ($R^2 = 0.98$) with a Stern−Volmer constant (K_{SV}) of 0.89 atm^{-1}.

Dissolved Oxygen in the Presence of Glucose Oxidase. In the presence of the enzyme glucose oxidase, β-D-glucose is oxidized by oxygen to D-glucono-1,5-lactone and hydrogen peroxide, with the glucose to oxygen stochiometry having a 1:1 ratio. Using a RBP-SZY-PDMS film, we monitored the emission of $Ru(bpy)_3^{2+}$ as different amounts of glucose (0, 0.25, 0.50, 0.75 and 1 mM) were added to a oxygen saturated solution containing glucose oxidase. These results are summarized in Table 1, which shows the estimates of the concentration of oxygen in solution based on the amount of glucose added, and the integrated emission intensity. Henry's law (Henry's Law constant = 1.3×10^{-3} mol atm^{-1} (dm^3)$^{-1}$) was used to estimate the concentration of dissolved oxygen of 40.3 ppm in a solution prepared by bubbling 1 atm O_2. The other oxygen concentrations in Table 1 were estimated from the glucose added. The emission intensities observed with the different glucose levels was also used to obtain the amount of dissolved oxygen, but by using the Stern−Volmer plot shown in Figure 4 ($I_o = 1.85 \times 10^9$ for a N_2-saturated solution of glucose using the same RBP−SZY−PDMS film). These oxygen concentrations are compared in Table 1 with those obtained based on the amount of glucose added, along with the percent differences.

Intracellular Oxygen Monitoring. RBP−SZY particles (∼500 nm) were used for monitoring intracellular oxygen in human monocyte-derived macrophages. Macrophages were chosen for their ability to internalize the RBP−SZY particles and for their ability to respond to various stimuli with a strong oxidative burst.

(21) Anderson, M. W.; Klinowski, J. *J. Chem. Soc., Faraday Trans. 1* **1986**, *82*, 1449–1469.
(22) Engelhardt, G.; Michel, D. *High-resolution solid-state NMR of silicates and zeolites*; John Wiley and Sons: Engelhardt, Germany, 1987.
(23) de Klerk-Engels, B.; Fruhauf, H. W.; Vrieze, K.; Kooijman, H.; Spek, A. L. *Inorg. Chem.* **1993**, *32*, 5528–5535.
(24) Black, D.; Deacon, G. B.; Thomas, N. C. *Aust. J. Chem.* **1982**, *35*, 2445–2453.
(25) Kelly, J. M.; O'Connell, C. M.; Vos, J. G. *Inorg. Chim. Acta* **1982**, *64*, L75–L76.
(26) Chardon-Noblat, S.; Da Costa, P.; Deronzier, A.; Haukka, M.; Pakkanen, T. A.; Ziessel, R. *J. Electroanal. Chem.* **2000**, *490*, 62–69.
(27) Demas, J. N.; Taylor, D. G. *Inorg. Chem.* **1979**, *18*, 3177–3179.

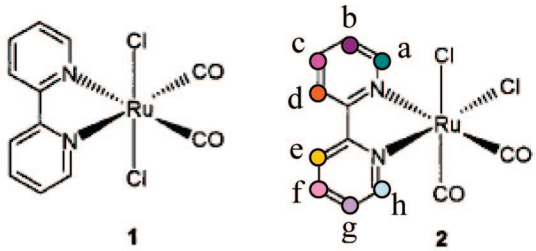

1 = trans (Cl) cis (CO)

2 = cis (Cl) cis (CO)

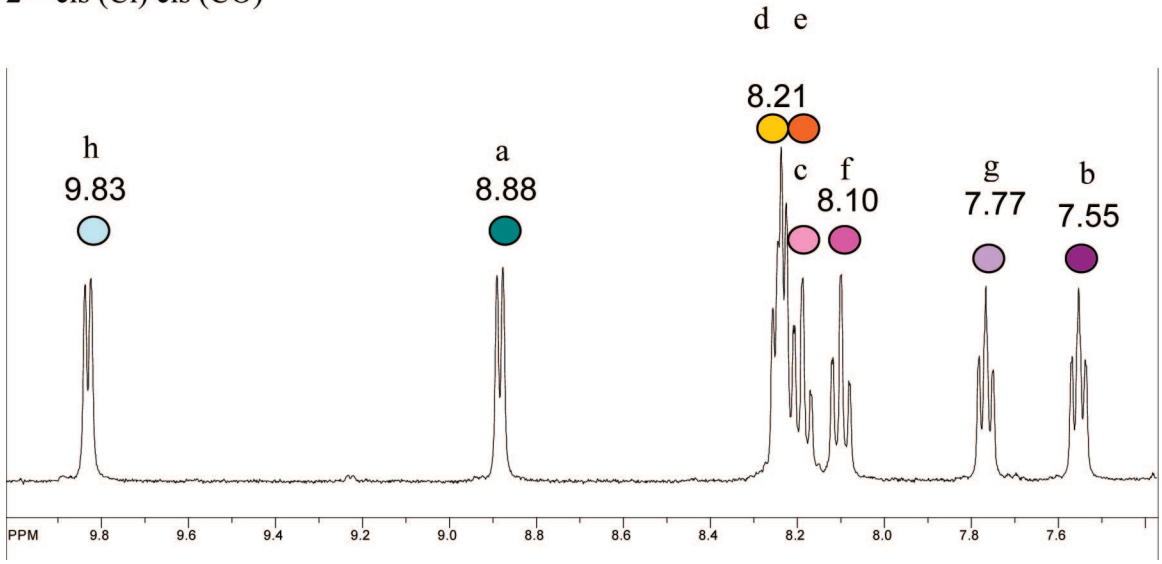

Figure 2. NMR spectrum of $RuCl_2(CO)_2(bpy)$. The NMR represents complex **2**, which is in the cis (Cl) cis (CO) conformation. The shades of the circles, as well as the letters, correlate the hydrogen atoms shown in the structure to the NMR peaks.

Scheme 1. Synthetic Scheme for Loading Tris(2,2′-bipyridyl) Ruthenium(II) Chloride Inside of Siliceous Zeolite-Y

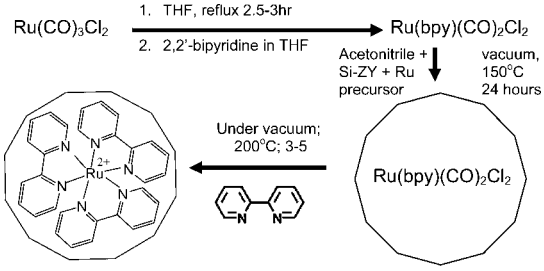

As part of the immune response, activated macrophages make reactive oxygen species with potent antibacterial activity. Our experimental strategy involved initiation of an oxidative burst in the RBP−SZY loaded macrophages, followed by monitoring of the emission from the RBP−SZY particles by confocal microscopy. In order to initiate the oxidative burst, we studied both zymosan and phorbol myristate as possible reagents. The kinetic profile of the zymosan and phorbol myristate-induced oxidative burst of macropahges was determined using a luminol assay which detects extracellular superoxide.[19,20] Figure 5 shows that zymosan induces a stronger oxidative burst, and that the peak of superoxide generation occurs ∼15 min after exposure to zymosan. Thus, zymosan was chosen to initiate the oxidative burst in subsequent experiments. Error bars represent standard deviations of mean luminescence values measured in triplicate wells.

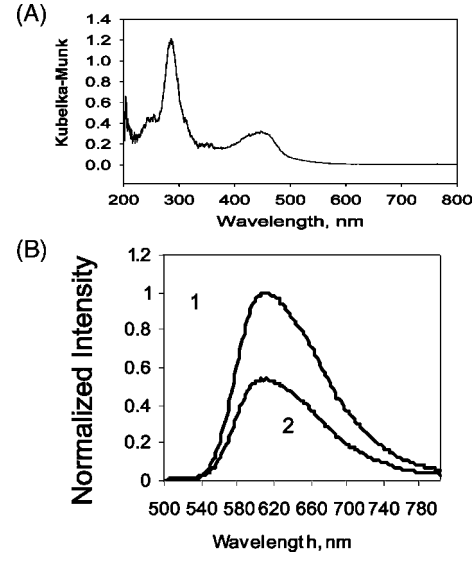

Figure 3. (A) Diffuse-reflectance UV absorption spectra of tris(2,2′-bipyridyl) ruthenium (II) loaded in siliceous zeolite-Y. (B) Luminescence intensity quenching with the top spectrum (1) representing nitrogen saturated water and the bottom spectrum (2) representing oxygen saturated water for a RBP−SZY−PDMS film.

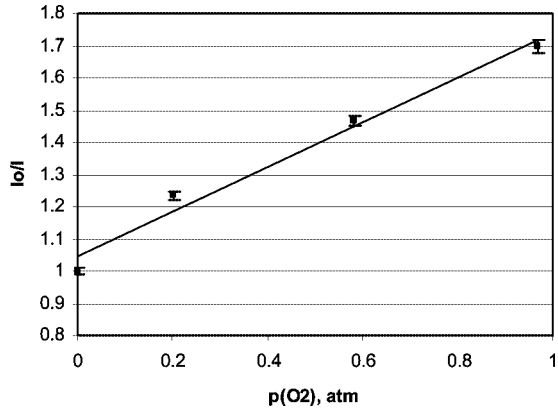

Figure 4. Stern−Volmer plot with gas saturated water solutions. $R^2 = 0.98$. $K_{SV} = 0.89$ atm^{-1}.

Table 1. Comparison of the Oxygen Concentration Calculated Stoichiometrically Based on Glucose/Glucose Oxidase Reactions to the Concentration of Oxygen Determined Using the Stern−Volmer Plot Equation (Figure 4)

Stern−Volmer calculated [O_2], ppm O_2	stoichiometrically calculated [O_2], ppm O_2	% difference
40.1	40.3	0.480
33.7	32.3	4.03
25.4	24.3	4.17
17.7	16.3	8.14
7.54	8.30	9.17

The macrophages in chamber slides were exposed to RBP−SZY particles and internalization of the particles was confirmed by confocal fluorescence microscopy by scanning through the z-plane. Several hours prior to microscopy the cells were also treated with the nuclear staining dye DAPI. Figure 6 shows a typical micrograph of a macrophage with RBP−SZY particles (red) and the blue nuclear stain. Considering that the zeolite particles are ~500 nm in size, it is obvious from Figure 6 that multiple zeolite particles were taken up by the macrophages. This is consistent with our previous electron microscopy studies of zeolite particles in macrophages.[28]

The RBP−SZY-loaded macrophages were then exposed to zymosan and the emission from the intracellular particles (and DAPI) was monitored over a 20-min time period by confocal

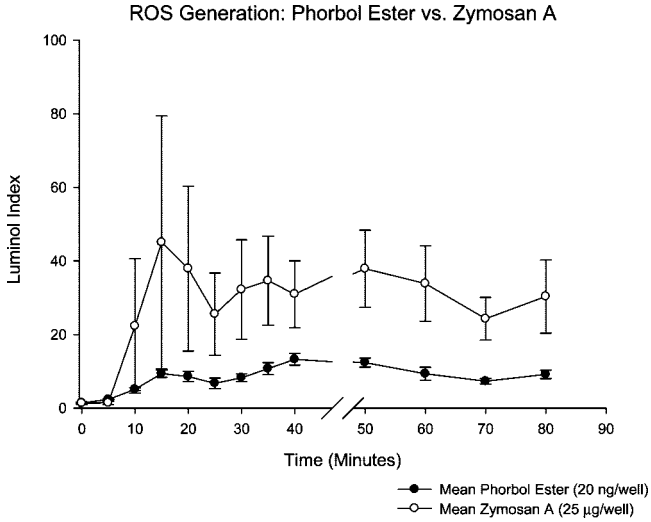

Figure 5. Results of luminol assay comparing the reactive oxygen species produced by phorbol 12-myristate 13-acetate and zymosan.

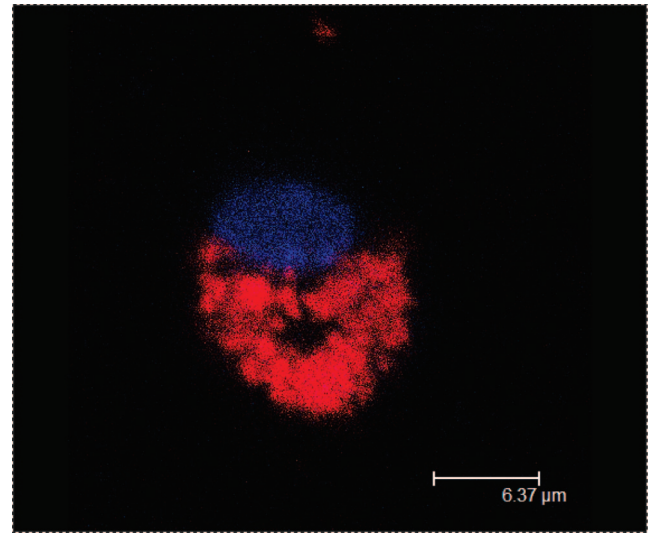

Figure 6. Confocal image of a macrophage after 24 h exposure to the ruthenium-loaded zeolite. The red area represents luminescence from the ruthenium-loaded zeolite and the blue area is from DAPI, a nuclear stain.

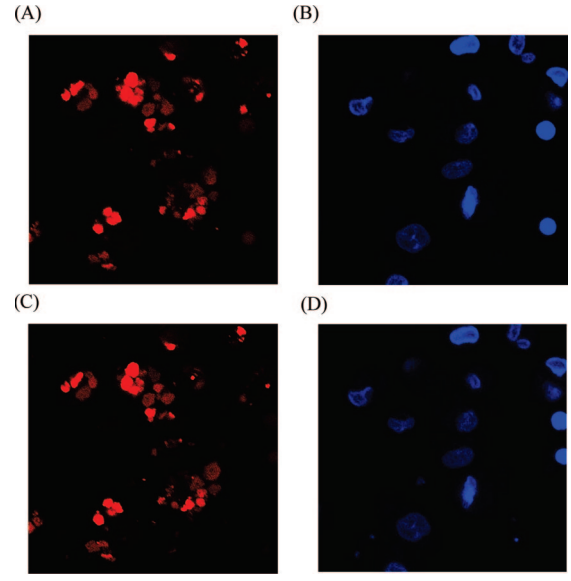

Figure 7. Confocal images as a function of time after induction of oxidative burst. (A) and (B) images are taken at 0 min. (A) depicts the luminescence of the ruthenium loaded zeolite while (B) depicts the luminescence from the DAPI stain. (C) and (D) images are taken at 20 min. (C) depicts the luminescence of the ruthenium loaded zeolite while (D) depicts the luminescence from the DAPI stain.

fluorescence microscopy. When these experiments were performed under an ambient atmosphere, no change in the emission signals (emission from $Ru(bpy)_3^{2+}$ normalized to DAPI) was observed following stimulation with zymosan. The experiments were then repeated under a CO_2 atmosphere. Precautions were taken not to expose the macrophages to the CO_2 environment for longer than 45 min, since cells exposed for an hour or longer exhibited morphologic changes suggestive of toxicity. Figure 7 shows the confocal images taken initially and after 20 min of incubation with zymosan. For data analysis, all completely visible cells (i.e., cells that were fully in the field being monitored and did not move out of frame during the scan) in the region were selected. Thus, for Figure 7, the seven cells that were in the middle of the micrograph (clear from the DAPI stain image)

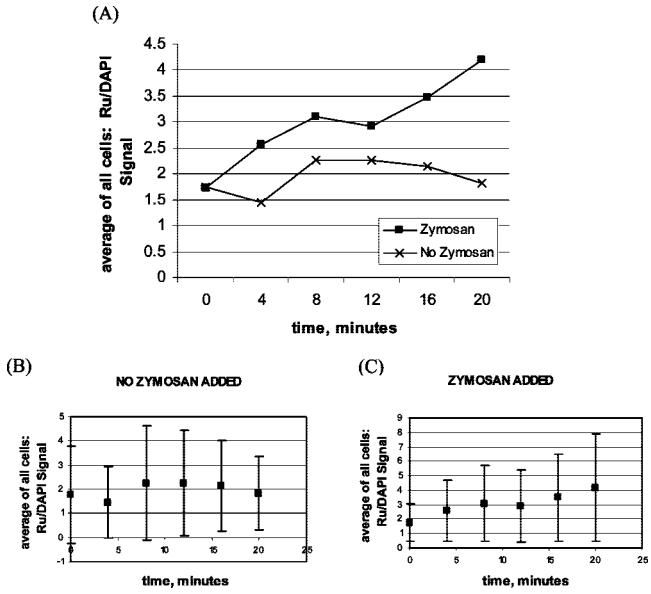

Figure 8. Plot of emission response to oxidative burst (A): The *y* axis is the ratio of the ruthenium complex fluorescence to the DAPI fluorescence. Each data point represent the average of 6−10 cells that were in the frame. The lower two plots represent the error bars for each data point. (B) represents the error bars for the data points where there was no addition of zymosan, and (C) represents the error bars for the data points where zymosan was added.

were used. It is clear that two cells on the extreme right side of the micrograph were moving out of the field and were not included. The luminescence intensity per cell was obtained for both the nuclear stain and the ruthenium complex. Figure 8a shows the change in average intensity of the seven cells over time, plotted as a ratio between the $Ru(bpy)_3^{2+}$ and DAPI emission. The emission ratio for a set of cells not exposed to zymosan is also shown in Figure 8a. The overall trend is increase of emission intensity from the RBP−SZY particles after exposure to zymosan. Increase of emission from $Ru(bpy)_3^{2+}$ indicates that the intracellular oxygen concentration is decreasing. Figure 8b shows the standard deviation of the emission ratio for both the zymosan-treated and untreated samples for the collection of cells. There is considerable variation in the emission from the different cells. Over the 20 min period the intensity of the $Ru(bpy)_3^{2+}$ emission normalized to DAPI is about two-fold. This experiment was repeated with MDM isolated from a second donor and the data is shown in Figure 3 in the Supporting Information.

Discussion

Synthesis of Ionic $Ru(bpy)_3^{2+}\cdot 2Cl^-$ Within Hydrophobic Siliceous Zeolite-Y. The ship-in-a-bottle synthesis, when used in conjunction with siliceous zeolite-Y, requires the use of a neutral ruthenium complex as a precursor. Previous attempts have used $Ru(bpy)Cl_3$ as a precursor in siliceous zeolite-Y due to its good solubility in organic solvents. However, $Ru(bpy)Cl_3$ is found in nonmonomeric forms,[29,30] and dimers and polymers will not penetrate through the windows of the supercages, possibly resulting in the low loading levels of the $Ru(bpy)_3^{2+}$ (1/10 000 supercages) that was reported previously.[14] The precursor used in this study, (2,2′-bipyridyl)dicarbonyldichloro ruthenium (II), $Ru(bpy)Cl_2(CO)_2$ is neutral, can be synthesized in nonpolymeric forms, and as demonstrated here lends itself to a ship-in-a-bottle synthesis with siliceous zeolite-Y for a variety of loading levels (1 $Ru(bpy)_3^{2+}$/7 and 25 supercages). To the best of our knowledge, this study is the first to report controlled loading of ionic species in hydrophobic zeolites.

Oxygen Quenching. Quenching of the emission of ruthenium and porphyrin-based dye by oxygen has been extensively studied in the literature. Of particular interest are the Stern−Volmer plots. For tris(4,7-diphenyl-1,10-phenanthroline) ruthenium(II) perchlorate immobilized in a silicone rubber matrix, a downward curvature of the Stern−Volmer plot was observed.[31] Pt and Pd octaethylporphyrins in three different polymers (ethyl cellulose, cellulose acetate butyrate polymer, or polyvinylchloride) led to nonlinear Stern−Volmer plots.[32] For tris(4,7-diphenyl-1,10-phenanthroline) ruthenium(II) immobilized in either n-triethoxysilane/tetraethylorthosilane composite films, a nonlinear Stern−Volmer plot was obtained.[33] A nonlinear Stern−Volmer for $Ru(bpy)_3^{2+}$ in aluminous zeolite-Y was also reported.[12] In our previous study of $Ru(bpy)_3^{2+}$ in siliceous zeolite using $Ru(bpy)Cl_3$ as the precursor, we reported a nonlinear Stern−Volmer plot.[14] The nonlinearity was due to the inhomogeneous distribution of $Ru(bpy)_3^{2+}$ due to the inability of the precursor to penetrate the entire intrazeolitic space, because of its polymeric nature.

Linear Stern−Volmer plots have been reported for organically modified silicate (ORMOSIL) hosts with ruthenium probes.[10,33–35] In Figure 4, we show a linear Stern−Volmer plot for the RBP−SZY sample. At the loading level of 1 $Ru(bpy)_3^{2+}$ per 25 supercages that we are examining in this study, the $Ru(bpy)_3^{2+}$ molecules are distributed within the zeolite with a very low probability of molecules being in neighboring cages.[36] Thus, each $Ru(bpy)_3^{2+}$ is isolated in a supercage and surrounded by empty supercages. The crystalline nature of the zeolite assures a reasonably uniform environment around each $Ru(bpy)_3^{2+}$ molecule. We propose that the homogeneous environment around the dye molecules is the reason for the linearity of the Stern−Volmer plot. Another reason for the lack of linearity in Stern−Volmer plots is inaccessibility of oxygen to all of the dye molecules in the host matrix.[37] The use of hydrophobic siliceous zeolite-Y promotes O_2 partition into the zeolite and low loading levels of $Ru(bpy)_3^{2+}$ ensure that movement through the zeolite cages is unimpeded. The linearity of the Stern−Volmer plot also suggests a dynamic quenching by oxygen,[4] this is expected since the intrazeolitic oxygen can diffuse through the supercages unimpeded.

Changes during the Oxidative Burst. The model biological system using glucose oxidase demonstrates that it is possible to monitor the oxygen concentrations in solution due to chemical changes. With knowledge of the emission in an oxygen-free environment, it was possible to estimate the dissolved oxygen concentrations from the Stern−Volmer plot (Table 1). The sample used in the glucose oxidase experiments was RBP-SZY particles dispersed in a PDMS film. The use of siliceous zeolite aids in

(28) Long, J. F.; Dutta, P. K.; Hogg, B. D. *Environ. Health Perspect.* **1997**, *105*, 706–711.
(29) Thummel, R. P.; Lefoulon, F.; Chirayil, S. *Inorg. Chem.* **1987**, *26*, 3072–3074.
(30) Kelch, S.; Rehahn, M. *Macromolecules* **1997**, *30*, 6185–6193.
(31) Bacon, J. R; Demas, J. N. *Anal. Chem.* **1987**, *59*(23), 2780–2785.
(32) Douglas, P.; Eaton, K. *Sens. Actuators, B* **2002**, *82*(2−3), 200–208.
(33) Tang, Y.; Tehan, E. C.; Tao, Z.; Bright, F. V. *Anal. Chem.* **2003**, *75*, 2407–2413.
(34) Pang, H. L.; Kwok, N. Y.; Chow, L. M. C.; Yeung, C. H.; Wong, K. Y.; Chen, X.; Wang, X. *Sens. Actuators, B* **2007**, *123*(1), 120–126.
(35) Chen, X.; Zhong, Z.; Li, Z.; Jing, Y.; Wang, X.; Wong, K. *Sens. Actuators, B* **2002**, *87*(2), 233–238.
(36) Sykora, M.; Kincaid, J. R.; Dutta, P. K.; Castagnola, N. B. *J. Phys. Chem. B* **1999**, *103*, 309–320.
(37) Hartmann, P.; Leiner, M. J. P.; Lippitsch, M. E. *Sens. Actuators, B* **1995**, *29*(1−3), 251–257.
(38) Li, L.; Walt, D. R. *Anal. Chem.* **1995**, *67*, 3746–3752.

oxygen transport from water into the zeolite, mainly because of the increased hydrophobicity, a fact that has been exploited with other hosts for optical oxygen sensing. The glucose oxidase assay has been utilized previously for glucose sensing.[38–41]

Macrophages are professional phagocytes and were used in this study as a model for living cells. Unlike the use of PDMS films for glucose oxidase, zeolite particles were used to monitor intracellular oxygen concentrations. Macrophages readily internalize the RBP-SZY particles (~500 nm) following the addition of particles to culture medium, and thus we did not have to resort to other forms of particle introduction. In addition, these cells are capable of producing an oxidative burst upon stimulus, which should lead to a decrease of intracellular oxygen,[42] demonstrating the feasibility of the zeolite-encapsulated dyes as intracellular oxygen sensors. Fluorescence microscopy demonstrates that the RBP−SZY particles within the cell are fluorescent, as shown in Figure 6.

Zymosan is a particulate stimulus; after binding to the macrophage and being internalized, NADPH-oxidase is activated inducing an oxidative burst.[43] As seen in Figure 5, the peak of the oxidative burst occurred within the first 15 min and is the time frame used in this experiment. The experiments performed in air showed no change of the emission of the RBP−SZY particles with the addition of zymosan. We propose that the extracellular oxygen in the air provides a constant supply of oxygen to the intracellular compartments of the macrophages.

Thus, macrophage responses were observed in a CO_2 atmosphere, with the precaution that cells were not exposed to CO_2 for more than an hour. The use of CO_2 atmosphere is not biologically relevant, but our goal in this study was to demonstrate whether we can monitor intracellular oxygen via the dye-loaded particles in a living cell. Figure 8B shows the emission ratio for a collection of cells that were not exposed to zymosan. Intracellular oxygen concentration is expected to remain relatively constant. The $Ru(bpy)_3^{2+}$/DAPI ratio remains relatively constant around ~2, but the standard deviations are large. This is attributed to the fact that each cell takes up different amounts of particles, so the average intensity for all cells show a large standard deviation. After zymosan addition, the average emission keeps increasing, as would be expected due to oxygen depletion in the cytoplasm. The standard deviation still remains large because of the unequal distribution of particles in the cells.

Though the data demonstrate that the dye-zeolite particles respond to changes in intracellular concentrations of oxygen, it is difficult to quantitate the amount of oxygen since the macrophages take up different amounts of particles. Also, in order to use the Stern−Volmer plot as was done for glucose oxidase, a value for intensity in a completely N_2 atmosphere is required and cell survivality with N_2-saturated cytoplasm was of concern. The data in Figure 8A suggest that at 20 min postexposure to zymosan, the intensity ratio has increased by a factor of 2, as compared to untreated cells. If we consider that the oxygen concentration in the cytoplasm at the start of the experiment is similar to air saturated solution, and at the peak of the oxidative burst all dissolved oxygen is depleted (resembling N_2-saturated solution), then the Stern−Volmer plot in Figure 2 would predict an increase of a factor of 1.25 as compared to a factor of 2 that is observed in the macrophage experiments.

Macrophages are inherently motile cells and thus have the potential to move during the observation period. Hence DAPI stain of the nucleus was used to normalize the data. The normalization is helpful to some degree, but cell movement and the confocal imaging of a narrow region along the *x* axis results in probing of a different part of the zeolite crystallites. This results in the lack of proper quantitative estimation of oxygen concentration from data in Figure 8.

Several studies have measured intracellular dissolved oxygen using a dye-host system, known as PEEBLE sensors.[9,10] These PEEBLE sensors of 50−300 nm in size were prepared by incorporation $(Ru(dpp)_3^2$ (dpp = diphenyl-1,10-phenanthroline) and oxygen insensitive dye (Oregon Greens 488-dextran) into a polyethylene glycol-silica matrix. The sensor particles were injected into rat C6 glioma cells and fluorescence spectra recorded from cells in air-saturated and nitrogen-saturated buffers. Using the ratiometric fluorescence ratio, and the I_o (N_2) value in solution, an intracellular oxygen concentration of 7.9 ± 2.1 ppm was found for cells in air-saturated buffers. In another study, PEBBLE sensors with Pt(II)octaethylporphine and Pt(II)octaethylporphine ketone have also been investigated successfully for measuring changes in intracellular oxygen concentration in C6 glioma cells due to respiration.

In extension of the previous PEBBLE work, we demonstrate in this paper that the dye-host particles can also monitor changes in oxygen concentration with a specific type of intracellular activity. In order to alleviate the quantitation problems, we are investigating the use of 20−30 nm sized zeolite particles, which should have a more uniform distribution in the cells. Because of the "solution-like" behavior of these nanoparticles, external calibration to obtain values of I_o becomes possible, as was done with the PEBBLE sensors. The advantages of the zeolite-based system are that the toxic dye will not leach from the matrix (these particles were subjected to Soxhlet extraction for 4 weeks and ion-exchange) and that interference from cellular contents will be minimized because of the 7 Å opening into the zeolite. Another advantage of zeolites as intracellular sensors is that with more aluminous zeolites, the transport of cations such as H^+, Na^+, K^+, Ca^{2+}, and transition metal ions into the zeolite is promoted via ion-exchange and with the appropriate dyes, can be developed into sensors.

Conclusions

By suitable choice of the neutral ruthenium precursor $Ru(bpy)Cl_2(CO)_2$, the loading level of the ionic species tris(2,2′-bipyridyl) ruthenium(II) in hydrophobic siliceous zeolite-Y could be increased to 1 ruthenium complex per 7 supercages. Using a sample with a loading level of 1 $Ru(bpy)_3^{2+}$ per 25 supercages dispersed in a PDMS film, the emission of $Ru(bpy)_3^{2+}$ as a function of dissolved oxygen was monitored. The Stern-Volmer plot was best represented as a linear curve ($R^2 = 0.98$). The concentration of the dissolved oxygen in solution was altered by addition of glucose in the presence of glucose oxidase. Estimates of the dissolved oxygen concentration were made by use of the Stern−Volmer plot and agreement within 5% of the values estimated from the added glucose was observed. The $Ru(bpy)_3^{2+}$-siliceous zeolite crystallites were incorporated into macrophages and shown to respond to changes in dissolved intracellular oxygen concentrations upon oxidative burst induced by zymosan when the cells were maintained in a CO_2 environment. The advantages of the dye-zeolite host system is that the probe is permanently encapsulated in a zeolite of submicron dimensions, with no possibility of dye leaching. The disadvantage for the intracellular measurement was that the macrophages took up different numbers

(39) Rosenzweig, Z.; Kopelman, R. *Sens. Actuators, B* **1996**, *35−36*, 475–483.
(40) Moreno-Bondi, M. C.; Wolfbeis, O. S. *Anal. Chem.* **1990**, *62*, 2377–2380.
(41) Pasic, A.; Koehler, H.; Klimant, I.; Schaupp, L. *Sens. Actuators, B* **2007**, *122*, 60–68.
(42) James, P. E.; Grinberg, O. Y.; Swartz, H. M. *J. Leukocyte Biol.* **1998**, *64*, 78–84.

of particles and so the averaged emission exhibited large standard deviations. Also, the quantitative measure of the intracellular oxygen was not possible because an estimate of the emission in an oxygen-free environment could not be obtained.

Acknowledgment. This material is based upon work supported by the National Science Foundation under IGERT Grant No. 0221678 and NIOSH Grant No. R01 OH009141 (P.K.D. and W.J.W.).

Supporting Information Available: NMR and IR spectra of the ruthenium precursor, as well as the results of the oxidative burst obtained from macrophages from a second human donor are shown. This material is available free of charge via the Internet at http://pubs.acs.org.

LA801204Y

(43) Pasmans, F.; De Herdt, P.; Nerom, A. V.; Haesebrouck, F. *Dev. Comp. Immunol.* **2001**, *25*, 159–168.